The potential of 1 h refractivity changes from an operational C-band magnetron-based radar for numerical weather prediction validation and data assimilation

RMetS
Royal Meteorological Society

The potential of 1 h refractivity changes from an operational C-band magnetron-based radar for numerical weather prediction validation and data assimilation[†]

J. C. Nicol,[a]* A. J. Illingworth[b] and K. Bartholomew[b]
[a]*National Centre for Atmospheric Science (NCAS), University of Reading, UK*
[b]*Department of Meteorology, University of Reading, UK*

*Correspondence to: J. C. Nicol, National Centre for Atmospheric Science (NCAS), University of Reading, Reading RG6 6BB, UK.
E-mail: j.c.nicol@reading.ac.uk

Refractivity changes (ΔN) derived from radar ground clutter returns serve as a proxy for near-surface humidity changes (1 N unit ≡ 1% relative humidity at 20 °C). Previous studies have indicated that better humidity observations should improve forecasts of convection initiation. A preliminary assessment of the potential of refractivity retrievals from an operational magnetron-based C-band radar is presented. The increased phase noise at shorter wavelengths, exacerbated by the unknown position of the target within the 300 m gate, make it difficult to obtain absolute refractivity values, so we consider the information in 1 h changes. These have been derived to a range of 30 km with a spatial resolution of ∼4 km; the consistency of the individual estimates (within each 4 km × 4 km area) indicates that ΔN errors are about 1 N unit, in agreement with *in situ* observations. Measurements from an instrumented tower on summer days show that the 1 h refractivity changes up to a height of 100 m remain well correlated with near-surface values. The analysis of refractivity as represented in the operational Met Office Unified Model at 1.5, 4 and 12 km grid lengths demonstrates that, as model resolution increases, the spatial scales of the refractivity structures improve. It is shown that the magnitude of refractivity changes is progressively underestimated at larger grid lengths during summer. However, the daily time series of 1 h refractivity changes reveal that, whereas the radar-derived values are very well correlated with the *in situ* observations, the high-resolution model runs have little skill in getting the right values of ΔN in the right place at the right time. This suggests that the assimilation of these radar refractivity observations could benefit forecasts of the initiation of convection.

Key Words: boundary-layer humidity; convective initiation; humidity

Received 24 June 2012; Revised 13 May 2013; Accepted 13 June 2013; Published online in Wiley Online Library 10 March 2014

1. Introduction

It has been generally acknowledged that water vapour is quite poorly represented in numerical weather prediction (NWP) models (Dabbert and Schlatter, 1996; National Research Council, 1998). Both the quantity and distribution of water vapour have a major influence on the prediction of mesoscale and storm-scale weather, particularly with respect to quantitative precipitation forecasting (Emanuel *et al.*, 1995; Fritsch *et al.*, 1998; Droegemeier *et al.*, 2000). Many studies have indicated the importance of obtaining low-level moisture variability in convection initiation (Weckwerth *et al.*, 1996; Koch *et al.*, 1997; Parsons *et al.*, 2000), though this variability is poorly characterized by existing observing platforms (Weckwerth *et al.*, 2004). Crook (1996) demonstrated that variations in boundary-layer temperature and moisture that are within typical observational variability (1 °C and 1 g kg^{-1}, respectively) can make the difference between no initiation and intense convection.

Initially proposed by Fabry *et al.* (1997), radar refractivity retrievals can provide spatially distributed near-surface moisture data, albeit over relatively limited areas (i.e. the radar ground clutter field). Refractivity changes are derived from the phase

---

[†]The copyright for this article was changed on 14 March 2014 after original online publication.

change detected from stationary targets (ground clutter); the ground clutter field is typically limited to a range of 50 km or so under standard propagation conditions. Radar signals travel more slowly as the refractive index (n) of the air increases. As a result, the measured phase from stationary targets will decrease in proportion to the range of the target and the refractivity change, $\Delta N[N = (n - 1) \times 10^6]$. At about 20 °C, a refractivity change of 1 N unit ($\Delta N = 1$) may be due to either a temperature change of about 1 °C or a relative humidity (RH) change of just 1%. In warm conditions, refractivity may be used as a proxy for the low-level moisture field (Weckwerth *et al.*, 2005).

Many studies have presented cases where refractivity data have shown boundaries or structures in the moisture field that may have played a role in storm initiation and have suggested that refractivity data assimilation may be useful. Sun (2005) studied the impact of radar refractivity observations from the NCAR S-Pol on the numerical prediction of storm initiation for an isolated storm observed during the International H2O Project (IHOP_2002), a field programme aimed at improving sampling of the atmospheric low-level water vapour. The assimilation of the low-level humidity inferred from the refractivity was found to enhance the moisture variability and hence the convection initiation. Weckwerth *et al.* (2005) analyzed refractivity fields derived from radar and concluded that they had potential for forecasting convection initiation. Montmerle *et al.* (2002) initialized the humidity field in the lowest model level from refractivity measurements and found this to increase the low-level humidity, permitting more vigorous storm development and improving agreement with subsequent precipitation observations.

There are many modelling studies of the moisture fields observed during IHOP_2002; Weldegaber *et al.* (2011) found that the representation of humidity below 750 mb improved (decreased by 0.6 g kg^{-1}) for one case when the horizontal grid length changed from 4 to 1 km. Xue and Martin (2006a, 2006b) found that for a model with 1 km grid length, the timing and location of dry line convective initiation was predicted with an accuracy of 25 km and 20 min; they were able to model horizontal convective rolls with aspect ratios between 3 and 7 and showed that the resultant localized forcing determined the exact location of convective initiation. In this article, we compare the size and magnitude of refractivity features that are modelled by different versions of an operational model with different horizontal grid lengths but are initiated with the same observations.

Fabry (2006) examined the spatial structure of radar refractivity observed during IHOP_2002 and found a typical change of 1.5 N units over 10 km along the direction of the wind and of 2.5 N units over 10 km perpendicular to the wind (their figure 3). This variability was partially attributed to the eastsoutheast–westnorthwest climatological refractivity gradient (0.1 N units km^{-1}) and a diurnal modification of about 1 N units over 10 km was observed (their figure 4).

Fabry *et al.* (1997) described how refractivity changes may be determined relative to a reference period lasting an hour or so when near-surface refractivity is homogenous and known. This allows the retrieval of absolute refractivity fields rather than fields of changes from subsequent scans. Radar refractivity has generally been applied to relatively long-wavelength (e.g. S-band; 10 cm wavelength) weather radar with frequency-stable transmitters (i.e. klystrons). Weckwerth *et al.* (2005) demonstrated that refractivity fields may be estimated relative to such reference periods over considerable periods of time (e.g. weeks or months) with errors of about 3 N units. More recently, Bodine *et al.* (2011) compared refractivity retrieved from the S-band NEXRAD radars with *in situ* observations over a period of several months and found errors of up to 30 N units. They suggested that scan-to-scan refractivity changes may be better suited for forecasting applications. However, their results could have been affected by spreading targets with adjacent range-gates having correlated returns (Nicol and Illingworth, 2013). At shorter

wavelengths, finding suitably quiescent reference periods becomes more difficult due to the increased sensitivity to refractivity changes.

Refractivity changes between two times based on a pair of targets along the same azimuth (at ranges r_A and r_B) are given by

$$\Delta N = -\frac{c}{4\pi f_{Tx}} 10^6 \frac{\Delta\phi_B - \Delta\phi_A}{r_B - r_A}. \tag{1}$$

Here, c is the speed of light in a vacuum and f_{Tx} is the transmitted frequency. Phase-change differences ($\Delta\phi_B - \Delta\phi_A$) are typically calculated by 'pulse-pair' processing (e.g. Skolnik, 1990, p 23.15) although changes are estimated between range-gates rather than between pulses for Doppler velocity estimates. Phase change aliasing or folding becomes a greater problem at shorter wavelengths. In the C band ($\sim$5 cm wavelength), phase changes decrease with range at a rate of $\sim 13° \Delta N^{-1}$ km^{-1}. To reduce the likelihood of aliasing, refractivity changes are estimated from closely located target pairs, typically from adjacent range gates. For the operational C-band radar data analyzed in this study with a 300 m range-gate spacing, the maximum unambiguous refractivity change is $|\Delta N|_{\text{folding}} \approx 44$ (neglecting the effects of phase-change noise).

At shorter wavelengths, phase-change noise ($\sigma_{\Delta\phi}$) is proportionally greater: a target displacement of just 14 mm (28 mm change in the two-way path) in the C band introduces 180° phase shift. In practice, observed phase changes are very noisy, with errors arising from millimetre-scale target motion, changes in the vertical gradient of refractivity in relation to target height variability (Park and Fabry, 2010) and also target location uncertainty relative to the centre of the range gate (Nicol *et al.*, 2013) when significant refractivity changes and/or magnetron transmitter frequency drifts (Δf_{Tx}) occur. The phase-change noise (in radians) due to target location uncertainty (even for perfectly stationary targets) is given in Eq. (2) based on eqs (14) and (17) of Nicol *et al.* (2013), where L is the range resolution and ΔF_{Tx} is the fractional transmitter frequency change in parts per million ($\Delta F_{Tx} = \Delta f_{Tx}/f_{Tx} \times 10^6$). The total phase-change noise at any given time combines the contribution due to target location uncertainty with other sources of noise such as target motion:

$$\sigma_{\Delta\phi} \approx \frac{2\pi L f_{Tx}|\Delta N + \Delta F_{Tx}|10^{-6}}{c}. \tag{2}$$

The range resolution is related to the pulse duration τ by $L = c\tau/2$. As such, radar refractivity retrievals in the C band using a magnetron transmitter are significantly more challenging, particularly with the relatively long pulse ($\tau = 2\,\mu$s; $L = 300$ m) currently used for scans at the lowest elevations in the UK, as target location uncertainty and the associated phase-change noise increase with pulse length. For the radar considered here, an extra 2° phase-change noise occurs for each part-per-million change in either the refractivity or the transmitter frequency. Even with the relatively moderate changes in near-surface refractivity in temperate climates such as in the UK, retrievals can fail over times as short as 1 h in the most extreme cases. As we shall see later, this tends to occur when large refractivity and frequency changes coincide and a significant contribution from target location uncertainty to the total phase-change noise (including target motion) occurs; an example for a contribution of $\sigma_{\Delta\phi} \approx 50°$ with $\Delta N \approx +15$ and $\Delta F_{Tx} \approx +10$ ppm ($\cong$ 60 kHz) is presented in section 3.2 for the radar considered here.

Given the limitations for absolute refractivity retrievals with magnetron-based C-band radars, in this article we shall investigate whether the information contained in retrievals of 1 h *refractivity changes* with about 4 km spatial resolution has the potential to improve the representation of near-surface humidity in NWP forecast models. This is achieved through the comparison of 1 h refractivity changes obtained from both radar retrievals and NWP model output with *in situ* observations from a surface weather station.
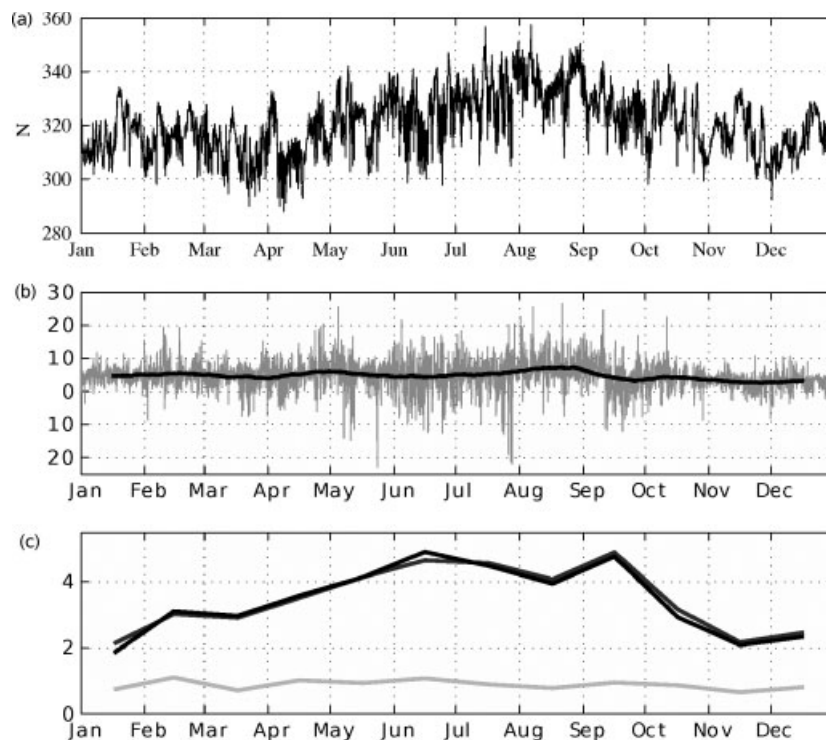
© 2013 The Authors. *Quarterly Journal of the Royal Meteorological Society* published by John Wiley & Sons Ltd on behalf of the Royal Meteorological Society.

Q. J. R. Meteorol. Soc. **140**: 1209–1218 (2014)

Figure 1. (a) Refractivity time series at Dunkeswell for 2008 based on hourly *in situ* measurements. (b) Refractivity difference between two stations Dunkeswell and Liscombe some 36 km apart. (c) Monthly standard deviation of refractivity differences between the two stations for N_d (light grey), N_w (dark grey) and N (black).

In section 2, we investigate the characteristics of near-surface refractivity derived from two meteorological surface stations operated by the Met Office and quantify the variability below the 4 km scale. The representativity of 1 h refractivity changes as a function of height is addressed using observations from a 200 m instrumented tower. Section 3 presents an outline of the radar refractivity retrieval algorithm applied to data from the UK operational network radar at Cobbacombe in Devon. Previous studies have estimated errors in the retrieved refractivity from comparisons with *in situ* measurements. We introduce a new method of estimating errors from the spatial consistency of the radar estimates, similar to the approach suggested in Fabry (2004). Both techniques indicate that 1 h refractivity changes can be derived with an accuracy of about 1 N unit. The representation of refractivity in the UK operational mesoscale forecast model (the Unified Model) run with various horizontal grid lengths (1.5, 4 and 12 km) is then discussed in section 4. One-hour refractivity changes from radar retrievals and model output are compared with *in situ* surface observations. Finally, general conclusions are presented in section 5.

2. *In situ* refractivity measurements

In situ measurements from two UK Met Office surface stations at Dunkeswell (altitude 252 m; ∼20 km southeast of the radar) and Liscombe (altitude 348 m; ∼20 km northwest of the radar) have been used for validation. Refractivity was derived from observations of temperature, T (K), pressure, p (hPa) and relative humidity (from which the partial water vapour pressure e (hPa) was derived) using the relation of Bean and Dutton (1968):

$$N = N_d + N_w = 77.6 \frac{p}{T} + 3.73 \times 10^5 \frac{e}{T^2}. \quad (3)$$

Here we refer to the dry (N_d) and wet (N_w) terms corresponding to the first and second terms respectively. Observations were made every minute at Dunkeswell, though only every hour at Liscombe.

2.1. Spatial and temporal refractivity variability

The refractivity time series at Dunkeswell during 2008 ranges between about 290 and 350 and exhibits a large degree of structure (shown in Figure 1(a)). Figure 1(b) shows the refractivity difference between the two stations every hour during 2008; the mean difference (in bold) of 4.6 N units throughout the year is consistent with a mean refractivity lapse rate of about 40 N units km^{-1}. Figure 1(c) depicts the monthly standard deviation of the differences between the two stations for the dry term (light grey), the wet term (dark grey) and the total refractivity (black).

The standard deviations of these differences are lowest during winter (∼2 N units) and largest during summer (∼4.5 N units). The mean and standard deviation of the difference between the stations throughout the year are 4.6 ± 3.7 (N), 2.6 ± 0.9 (N_d) and 2.0 ± 3.8 (N_w). The standard deviations of the differences in the dry term are rather small and quite constant throughout the year (<1 N unit). Almost all of the variability in these differences between the two stations is due to the wet term.

2.2. Spatial variability at scales below 4 km

Radar refractivity changes presented in this article have a spatial resolution of about 4 km, as a result of the smoothing required to obtain reliable retrievals, so we shall now consider the temporal variability measured at a surface station corresponding to scales below 4 km. The mean 10 m wind speed at Dunkeswell throughout 2008 was 4.5 m s^{-1}, implying that 4 km corresponds to a period of about 15 min for the advection of air past the surface station. The refractivity observations taken every minute at Dunkeswell have been examined to quantify the temporal variability and estimate the spatial variability of refractivity. A typical 24 h time series for the summer (6 July 2008), shown in Figure 2, illustrates the high-frequency variations occurring during sunny days, with minute-to-minute fluctuations reaching 3 N units. The standard deviation of the minute-to-minute refractivity values with respect to a 15 min running mean was calculated as a measure of the variability of the near-surface refractivity on scales below 4 km. The root-mean-square (rms) values of this variability as a function
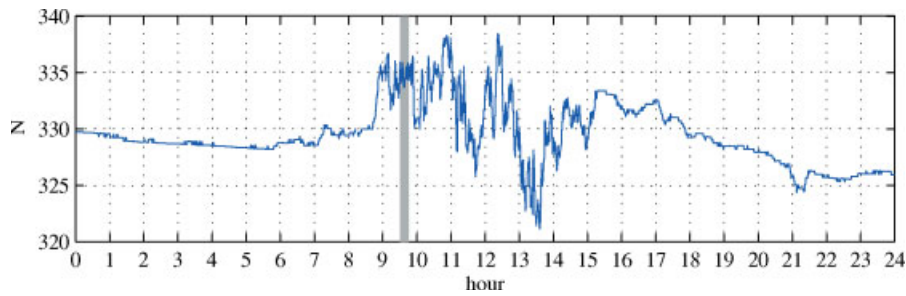
Figure 2. Refractivity time series from *in situ* measurements at Dunkeswell on 6 July 2008. A 15 min window used to estimate variability at scales below 4 km is shaded grey. This figure is available in colour online at wileyonlinelibrary.com/journal/qj

of time of day are shown in Figure 3 for winter (JF) and summer (JJ) 2008, highlighting the extremes of the average diurnal cycle throughout the year. To improve the representativity of 'point' *in situ* measurements relative to NWP models, this suggests that instantaneous observations of humidity (or refractivity), in particular, should be smoothed in proportion to the model grid length for comparison with or assimilation into forecast models. For a mean advection speed of $\sim$4.5 m s^{-1}, smoothing over approximately 6, 15 and 45 min would be appropriate for model grid lengths of 1.5, 4 and 12 km respectively.

The sub 4 km fluctuations are approximately 0.4 and 1.4 N units on average in winter and summer, respectively. The instantaneous differences between two stations due to these fluctuations would then be higher by a factor of $\sqrt{2}$ with values of approximately 0.6 and 2.0 N units in winter and summer. Comparing this with the corresponding rms differences (Figure 1(c)) of about 2 and 4.5 N units suggests that a significant fraction of the variance between the stations (36 km apart) can be attributed to scales above 4 km. It is this variability, largely due to humidity differences, that we hope to capture from the radar refractivity retrievals.

2.3. Vertical representativity of 1 h refractivity changes

Radar refractivity retrievals correspond to changes at a height above the surface dependent on the ground targets illuminated by the radar. The effective measurement height will naturally lie somewhere between the height of these ground clutter targets and the ground itself, which contributes to some of the radar returns. Observations of temperature, pressure and humidity made on a 200 m meteorological tower at Cabauw in the Netherlands (51.97°N, 4.93°E) have been used to investigate the relationship between 1 h *refractivity changes* as a function of height, thus extending the work of Weckwerth *et al.* (2005) who looked at the correlation of absolute refractivity values with height. These data, from a location with a similar climate to southern England, are provided every 10 min and correspond to the mean values of these quantities during the preceding 10 min period rather than being instantaneous observations.

The correlation between 1 h *refractivity changes* ($\rho_{\Delta N}$) at 10, 20, 40, 80, 140 and 200 m have been calculated relative to near-surface changes (at 1.5 m) using data covering the period

1 January 2002–31 August 2006. Figure 4(a) shows that the correlation between near-surface changes and those up to 40 m is over 0.9 during daylight hours in summer. Even at 200 m, the correlation is about 0.65 on summer days and greater than 0.8 on summer afternoons, when mixing in the boundary layer is greatest and correlations are highest. During the night throughout the year these correlations drop down to just 0.7 (not shown). On winter nights with light winds (<1 m s^{-1}), the correlations are lowest and observations at a height of 40 m are uncorrelated with 1 h changes near the surface (Figure 4(b)). Despite the poorer correlations at night, the high correlations observed during the day suggest that radar refractivity changes should be representative of near-surface changes and indeed over a 100 m layer above the surface. The main application of the refractivity observations is expected to be in improving forecasts of surface-driven convection: it is only daytime measurements, and those in summer in particular, that are of interest. The correlation between the absolute refractivity near the surface (1.5 m) and at 200 m was 0.94 on summer days and 0.96 on summer afternoons. These results correspond closely with the correlations (0.89–0.95) presented in Weckwerth *et al.* (2005) from the southern Great Plains during IHOP_2002 between *absolute* radar refractivity and aircraft observations at comparable heights ($\sim$200 m) in the boundary layer. They concluded that, under most daytime summer conditions, absolute near-surface refractivity is representative of a 250 m deep layer.

3. Radar refractivity retrieval

The algorithm implemented to retrieve 1 h refractivity changes from an operational C-band weather radar is briefly described in this section. We focus on differences with respect to the formulation presented by Fabry (2004), necessitated by the more severe phase-change noise due to the relatively short wavelength and magnetron frequency drifts of the radar used in this study. Refractivity data have been collected by the radar at Cobbacombe in southwest England covering the period March–August 2008: the absolute phase and the power ratio (e.g. Hubbert *et al.*, 2009) were recorded at each range gate in addition to the local oscillator frequencies for the lowest operational scan (0° elevation) every 5 min. A relatively long pulse was employed for these scans (2 μs;
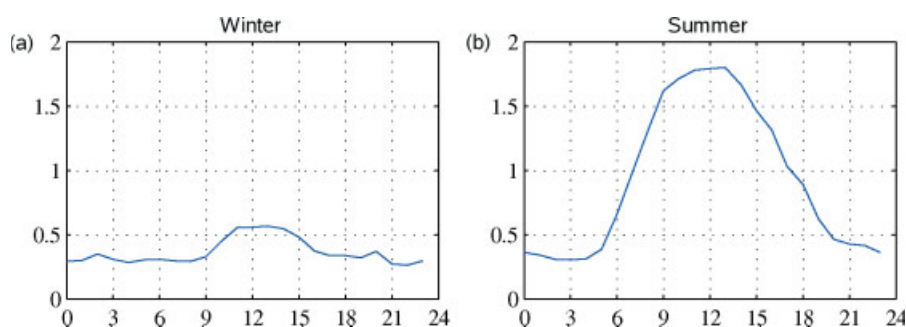

Figure 3. Root-mean-square refractivity variability below the 4 km scale, as a function of time of day in (a) winter (January–February 2008) and (b) summer (June–July 2008) at Dunkeswell. This figure is available in colour online at wileyonlinelibrary.com/journal/qj
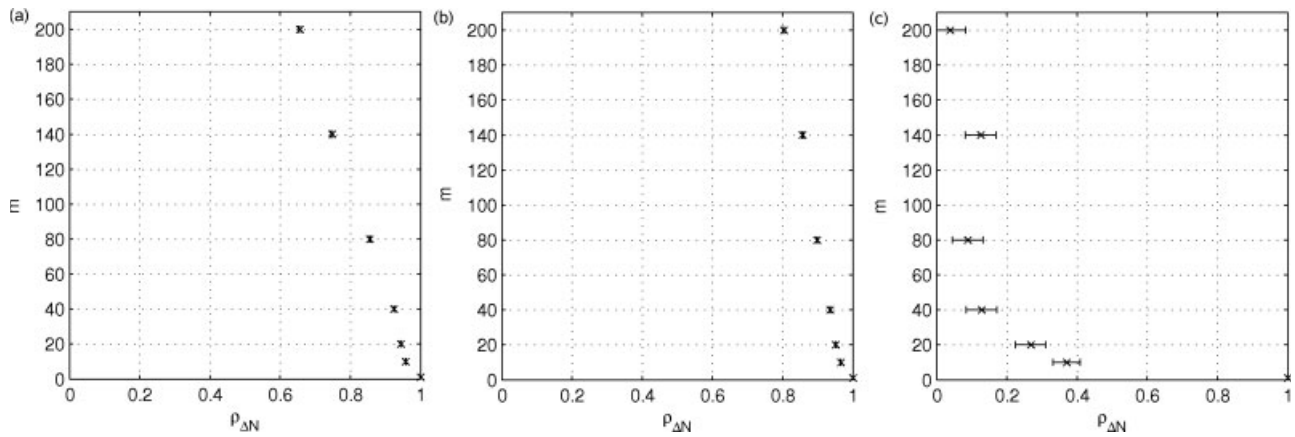
Figure 4. Correlation of 1 h refractivity changes at various heights on the Cabauw tower with observations at 1.5 m, from 2002–2006 for (a) summer daytime, (b) summer afternoons and (c) winter nights with light winds (<1 m s^{-1}).

300 m range resolution) with a pulse repetition frequency (PRF) of 300 Hz and a scan rate of 1.2 rpm (7.2 s^{-1}).

3.1. Outline of the radar refractivity retrieval algorithm

3.1.1. Stationary targets

To identify suitably stationary targets using an S-band radar, Fabry (2004) derived indices based on both real-time measurements (e.g. velocity and spectral width) and 5 min phase differences from a calibration period. This calibration period, lasting a few hours, should ideally correspond to windy conditions with negligible refractivity changes, but such conditions are progressively harder to meet at shorter wavelengths. For example, $\Delta N = 1$ over a 20 km path in 5 min corresponds to phase changes of about 140, 260 and 460° in S, C and X bands. Accordingly, in the C band we have used a single real-time parameter, the power ratio (PR), which represents the consistency of the returned signal at a particular range-gate in terms of both phase and amplitude, as the radar scans through each degree in azimuth. Nicol *et al.* (2012) demonstrated an excellent separation of clutter and precipitation echoes using PR for operational radars in the UK scanning at 1.2 rpm.

3.1.2. Frequency correction

Automated frequency control in radar systems with magnetron transmitters requires the adjustment of the frequency of local oscillators to follow the transmitter frequency. This requires adjustments to two local oscillators for the radar considered here. Occasional frequency adjustments of the stable local oscillator (STALO) are applied to maintain an intermediate frequency (IF) within 100 kHz of the nominal value (30 MHz). In addition, the frequency of the numerically controlled oscillator (NCO) is set prior to each scan for accurate down-conversion from IF to baseband. Local oscillator frequency changes lead directly to refractivity errors if a simple range-dependent correction (proportional to any changes in the sum of the local oscillator frequencies) is not applied (Nicol *et al.*, 2013). Nicol *et al.* demonstrated that the residual refractivity errors following correction for local oscillator frequency changes were less than 0.25 N units for the radar at Cobbacombe.

3.1.3. Field-averaged refractivity subtraction and phase-change smoothing

In refractivity retrievals, the field-averaged refractivity change ($\langle\Delta N\rangle_{\text{field}}$) is estimated and the effect of $\langle\Delta N\rangle_{\text{field}}$ is then subtracted from the observed phase changes. This is done so that less folding of the phases occurs and also to reduce the underestimation of refractivity changes relative to $\langle\Delta N\rangle_{\text{field}}$ which

result from the subsequent smoothing of phase changes (Nicol and Illingworth, 2013). Based on simulations in the S band, they recommended that a linear least-squares fit applied to the azimuthally averaged phase changes should be used when estimating $\langle\Delta N\rangle_{\text{field}}$ for radars with klystron transmitters. This was shown to avoid biases due to the presence of phase-correlated returns, which can occur when radar returns from ground targets spread over several range gates due to the length of the transmitted pulse and the filtering in the radar receiver. Nicol *et al.* (2013) showed that these phase-correlated returns tend to bias refractivity retrievals towards the fractional transmitter frequency change (ΔF_{Tx}). Because of the increased phase-change noise in the C band and the effects of magnetron frequency drift, we have obtained more accurate results by smoothing the phase-change data before calculating $\langle\Delta N\rangle_{\text{field}}$ using the standard pulse-pair processing. Although $\langle\Delta N\rangle_{\text{field}}$ may then be moderately underestimated, the final estimates of the 1 h refractivity changes have proved more accurate with this approach. The smoothing kernels were Gaussian functions (truncated at three standard deviations) in both range and azimuth (standard deviations: 375 m range; 750 m azimuth). The extent of the smoothing kernel with respect to range (acting as a low-pass filter on the measured phase changes) must be restricted to avoid large underestimates, particularly in local perturbations of refractivity changes and at shorter wavelengths (Nicol and Illingworth, 2013). However, this requires a delicate trade-off to ensure a sufficient reduction in phase-change noise.

3.1.4. Refractivity estimation

Biases due to phase-correlated returns and the effects of phase-change noise in general are reduced when the distance between targets used to estimate refractivity changes using Eq. (1) increases. Although this reduces the maximum unambiguous refractivity change from $|\Delta N|_{\text{folding}} \approx 44$ to ≈ 15, a three-gate separation has been found to provide the most accurate retrievals in comparison with surface observations. Local refractivity changes are estimated by smoothing estimates from each pair of targets, again using a Gaussian function truncated at three standard deviations, though of equal width in range and azimuth (standard deviation: 1500 m). To afford direct comparisons with model output, radar refractivity changes have also been averaged on to regular 4 and 12 km Cartesian grids.

3.2. Time series from accumulated refractivity changes

Figure 5(a) shows time series from *in situ* refractivity observations at Dunkeswell and from accumulating the corresponding 1 h radar refractivity changes during April 2008. There is no intention to derive refractivity changes over long periods of time by accumulating changes, as estimation errors will progressively develop in time, but these accumulations can be informative
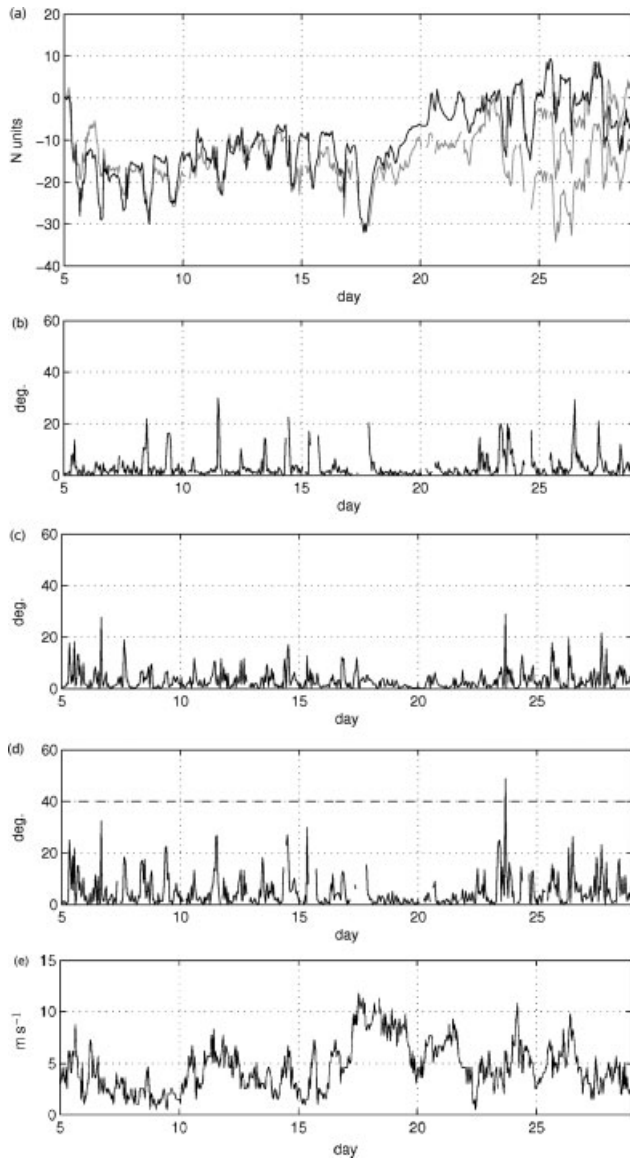
© 2013 The Authors. *Quarterly Journal of the Royal Meteorological Society* published by John Wiley & Sons Ltd on behalf of the Royal Meteorological Society.

Q. J. R. Meteorol. Soc. **140**: 1209–1218 (2014)

Figure 5. (a) Time series of accumulated ΔN at Dunkeswell from all available 1 h radar retrievals from 5–29 April 2008 (lower grey trace) and when the single refractivity change corresponding to large target location phase-change noise on 23 April is excluded (upper grey trace). Refractivity from *in situ* observations relative to the start of the time series is shown in black and smoothed over 15 min to reduce fluctuations below the 4 km scale. The two components of the target location phase-change noise due to (b) transmitter frequency changes and (c) refractivity changes (based on *in situ* data from Dunkeswell) are shown, along with (d) the total of these two components. (e) Ten-metre wind speeds at Dunkeswell are also shown.
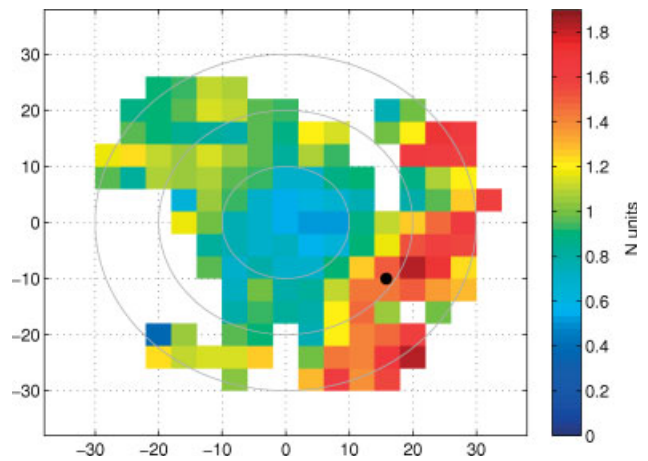

Figure 6. Root-mean-square retrieval errors in 1 h refractivity changes derived from the variability of the individual estimates within the averaging area (∼4 km × 4 km) during the period March–August 2008. The meteorological station at Dunkeswell is marked by a black dot.

dubious retrieval and reliable retrievals have been obtained at other times when similar or greater wind speeds have occurred.

3.3.   Radar refractivity retrieval errors

To provide real-time estimates of radar refractivity errors, we propose the following approach using the standard deviation of refractivity changes estimated from all pairs of targets encompassed by the smoothing kernels used to derive the mean refractivity changes. Because estimates from individual target pairs are not independent, due to phase-change smoothing, the number of independent target pairs (N_I) is derived from the ratio of the areas of the refractivity and phase-change smoothing kernels (i.e. $N_I = 8$). Refractivity retrieval errors are then equal to the standard deviation of refractivity changes from all target pairs divided by the square root of N_I. Figure 6 shows the rms retrieval error in 1 h refractivity changes during the period March–August 2008 in the region surrounding Cobbacombe, averaged on to a 4 km grid.

Retrieval errors are typically about 0.7 N units within 10–15 km of the radar and increase to about 1.0 N units to the northwest and about 1.4 N units to the southwest of the radar. These differences appear to be related to differences in target motion across the ground clutter domain, as this pattern closely resembles the spatial pattern of the average power ratio (not shown). Changes in the vertical refractivity gradient, combined with target height variability (Park and Fabry, 2010), result in phase-change noise that increases in proportion to range and is also likely to have contributed to this error pattern.

These retrieval errors have been evaluated from the divergence between *in situ* observations and accumulated radar time series over 24 h periods. To minimize representativity errors from the 'point' *in situ* observations, these divergences were calculated relative to midnight when temporal (and spatial) variability in the refractivity fields are typically lowest (for example, see Figure 2). Over a five-month period (March–August 2008), the rms 1 h retrieval error at Dunkeswell was estimated to be 1.38 N units (in accord with Figure 6). Based on the rms divergence of 24 h radar accumulations with respect to *in situ* observations (6.1 N units) and assuming that the retrieval errors from hour to hour were independent, the rms retrieval error in 1 h changes was determined to be 1.25 N units.

4.   Refractivity representation in Met office forecast models

The Met Office Unified Model solves non-hydrostatic, deep-atmosphere dynamics using a semi-Lagrangian numerical scheme (Davies *et al.*, 2005). In 2008, versions of the Unified Model were routinely run with horizontal grid lengths of 12 km (North

in evaluating the quality of radar retrievals. It may be seen that the comparisons over the initial two-thirds of the series are remarkably good in general, though a significant divergence between the series occurs on 23 April depending on whether a single questionable retrieval is included or not. In Figure 5(b) and (c), the phase-change noise due to target location uncertainty has been calculated for each term in Eq. (2) using 1 h changes in the transmitter frequency and *in situ* refractivity from the station at Dunkeswell respectively. The total target location phase-change noise is shown in Figure 5(d). The divergence between the series in Figure 5(a) coincides with the largest target location phase-change noise (>40°), when significant refractivity and transmitter frequency changes combine. Eliminating this estimate from the time series demonstrates improved agreement with *in situ* measurements in Figure 5(a). The contribution to the total phase-change noise due to target motion typically increases with wind speed (Fabry, 2004). Measurements of the 10 m wind speed at Dunkeswell (shown in Figure 5(e)) indicate that this contribution was likely to be only moderate at the time of the

Atlantic European: NAE) and 4 km (UK4). In addition, a high-resolution (1.5 km grid length) version (SUK) was under development and run on an occasional basis over the southern United Kingdom. The configurations of the models were generally very similar; the major difference being that the 1.5 km model was run without a convection parametrization and that the 4 km model had the parametrization modified to greatly reduce the convective mass flux. A summary of the differences in configuration between these models is presented in appendix A of Lean *et al.* (2008). However, for the model runs presented here, the number of vertical levels had also been increased from 38 to 76 in the 4 km model and, unlike the results presented by Lean *et al.*, the full operational data-assimilation system was used. The representation of refractivity in the NAE and UK4 models has been assessed by considering data in two 10 day periods: the 'spring' period (1–10 March 2008) and the 'summer' period (25 July–3 August 2008). SUK output from two active convective days in summer (27 and 28 July 2008) has also been analyzed.

4.1. Model characteristics – lowest three levels

The lowest three vertical levels in these models essentially follow the terrain at heights of 10, 49 and 127 m for the NAE and 5, 21 and 45 m for the UK4 and SUK. As radar retrievals are likely to correspond to heights of 5 m or less above the surface, the lowest model levels are most suitable for comparison. However, in locations with tall ground targets such as electricity pylons, measurements may be representative of higher levels. The rms refractivity differences between the lowest model levels and at levels close to 50 m (level 2 in the NAE and level 3 in the UK4) were 0.4 N and 1.1 N units in the spring and summer periods for the NAE and 0.3 N and 1.0 N units respectively for the UK4. Such differences are consistent with a refractivity lapse rate of 35–40 N units km^{-1}, particularly if the representativity errors based on this may conceivably reach 1 N unit. In any case, these differences are unlikely to be significant in view of the 1 N unit errors in the radar refractivity estimates.

4.2. One-hour refractivity changes

One-hour refractivity changes for the various grid-length models have been compared with *in situ* surface observations at Dunkeswell, which were available every minute though smoothed to reduce structures at scales below 12 km. The UK4 model has been averaged on to a 12 km Cartesian grid before refractivity changes are calculated to afford a fair comparison. Larger changes are typically observed between different forecast runs of the models at the transition between forecasts and subsequent analyses, particularly during summer (Bartholomew, 2012). These transitions occur at different times for the UK4 and NAE models, so only data avoiding these transitions have been included in the following analysis. The rms 1 h changes from *in situ* observations were 2.0 and 2.8 N units based on 151 and 160 1 h changes for the spring and summer 10 day periods, respectively. This compares with 1.9 and 2.0 N units (NAE) and 1.9 and 2.3 N units (UK4) during these periods. Therefore, the magnitude of the refractivity changes represented in both the UK4 and NAE was in close agreement with *in situ* observations during the spring period. During the summer period, the magnitude of these changes was underestimated in both models, to a greater degree in the NAE. The larger changes from the *in situ* observations during summer can be explained in part by the fact that smoothing the surface observations effectively reduces the along-wind component of small-scale fluctuations, though not the cross-wind fluctuations (which are typically larger), which will not be resolved in the models. These small-scale fluctuations are larger in summer, as the warmer temperatures lead to greater variability in absolute humidity. Despite this, the NAE seems to be underestimate humidity variability at the grid-length scale (12 km).

Table 1. Median decorrelation lengths (km) for refractivity (N), temperature (T), partial vapour pressure (e) and pressure (p) estimated from the NAE, UK4 and SUK models over two convective days (27 and 28 July 2008).

	N	T	e	p
NAE	24	24	24	43
UK4	16	20	18	29
SUK	12	19	15	36

The rms 1 h changes in the wet term (N_w) were within 0.1 N units of the rms 1 h total refractivity changes in *in situ* observations for both models during both periods, again indicating that refractivity changes are dominated by changes in N_w. This suggests that a forward operator based solely on N_w may be adequate concerning data assimilation of refractivity changes in NWP models.

4.3. Structures represented by the Met Office Unified Model

Model output from two convective summer days (27 and 28 July 2008) was available at all three model resolutions. Figure 7 compares refractivity changes between 0300 and 0600 UTC on 28 July 2008 with respect to 0000 UTC on 28 July 2008 in the NAE, UK4 and SUK models. Also shown at these times are the *accumulated* 1 h radar retrievals, also with respect to 0000 UTC. It is clear that, as the grid length becomes shorter, the model fields show progressively more small-scale structure and the magnitude of changes increases.

Decorrelation lengths have been derived from *absolute* refractivity fields for all three models based on these two summer days. Two-dimensional correlations of these fields were calculated and the decorrelation length was taken from the axis along which the most rapid decorrelation was observed (i.e. from the minor axis of the 2D correlations). The median decorrelation lengths are shown in Table 1 to the nearest kilometre, along with those for temperature (T), partial vapour pressure (e) and pressure (p). Although the decorrelation scales for temperature are only slightly changed at different grid lengths, the scale over which refractivity decorrelates is halved going from NAE to SUK models. Strongly associated with the humidity field, the refractivity decorrelation lengths correspond to 2, 5 and 8 grid lengths in the NAE, UK4 and SUK models respectively. Lean and Clark (2003) determined that features seen in the Unified Model at scales below about five grid lengths are likely to be attenuated by the closeness of their scale to the model grid length. This suggests that the refractivity structures represented in these models would only be well represented in the case of the SUK and perhaps to a lesser extent the UK4.

4.4. Time series of 1 h refractivity changes

To compare the observed radar-derived refractivity changes with the representation of refractivity in the forecast models over the 'spring' and 'summer' periods, all data have been averaged on to a common 12 km Cartesian grid. Time series of 1 h refractivity changes from a day selected from each of these periods (2 March 2008 and 1 August 2008) are shown in Figure 8; radar-derived changes (red) and those derived from model output from the UK4 (green) and NAE (blue) are compared with surface observations at Dunkeswell. Again, changes between model runs have been excluded from the analysis. The comparison between radar and surface observations is very good, particularly on 2 March. In contrast, the model comparisons are rather poor, particularly considering that the surface observations used here for comparison were assimilated in these models. To demonstrate that these two days are not exceptions to the general trend, the correlations between the 1 h changes have been calculated for each day of the spring and summer periods and are displayed in Figure 9(a) and (b), respectively. Time series from the two days shown in Figure 8 each contribute a single point to the series
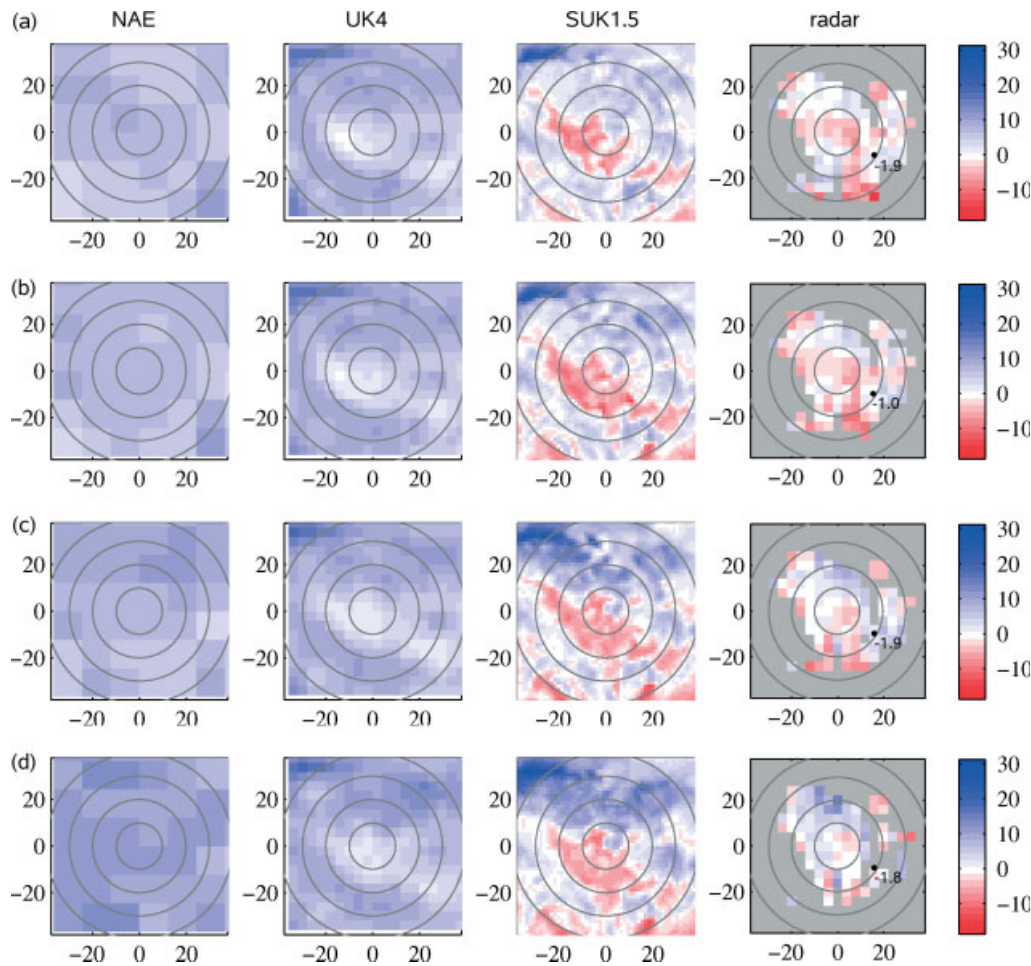
© 2013 The Authors. *Quarterly Journal of the Royal Meteorological Society* published by John Wiley & Sons Ltd on behalf of the Royal Meteorological Society.

Q. J. R. Meteorol. Soc. **140**: 1209–1218 (2014)

Figure 7. Refractivity changes (in *N* units) with respect to 0000 UTC on 28 July 2008 in the NAE (12 km grid length), UK4 (4 km grid length) and SUK (1.5 km grid length) models (left to right), at (a) 0300 UTC, (b) 0400 UTC, (c) 0500 UTC and (d) 0600 UTC on 28 July 2008. Shown in the rightmost column are the corresponding radar refractivity changes accumulated from 0000 UTC and changes based on *in situ* observations at Dunkeswell (black dot). As the model grid length decreases, the size of the features more closely resembles those derived from the radar.

of correlation coefficients in Figure 9(a) and (b). Again, 95% confidence intervals are shown based on the correlation and the number of points in each series.

The agreement between radar and *in situ* observations in Figures 8 and 9 is consistently better than the agreement between models and surface observations. This indicates that, even if the model is representing refractivity features at a smaller scale (closer to the scale of structures depicted by the *in situ* observations), the model does not necessarily get features in the right place at the right time. The agreement between both data sets is better during the spring period than during the summer period, suggesting that more significant fluctuations occur at small scales during summer (see section 2.2) and result in poorer agreement with the other datasets. A more thorough analysis has shown that temperature and pressure changes are typically well-captured in the models and the poor representation of humidity changes in the model is the cause of the lower correlations shown in Figure 9.

5.   Conclusions

Refractivity time series derived from instantaneous *in situ* measurements of temperature, pressure and humidity show a significant degree of variability at small scales (e.g. < 4 km). These fluctuations are highest on days in summer with clear skies, when the standard deviation of these fluctuations reaches about 3 *N* units. Although surface observations made with high temporal resolution may be smoothed to reduce this variability, this essentially reduces the along-wind fluctuations but not the cross-wind fluctuations, which are not resolved by either radar retrievals or model fields. Fabry (2006) demonstrated that refractivity fields are in fact more variable in the cross-wind than

in the along-wind direction. Instantaneous surface observations of humidity (or refractivity) should be averaged appropriately if they are to be assimilated in NWP models; the averaging should be determined by the typical time taken to advect an air mass over the model grid length.

Observations from an instrumented meteorological mast show that 1 h *refractivity changes* up to a height of about 100 m are representative of those made near the surface on summer days. Significant differences with height occur when the atmosphere near the surface becomes stably stratified, but such occasions are of little importance regarding the initiation of surface-driven convection.

Due to the relatively short wavelength and long pulse of the radar considered, in conjunction with frequency drifts from the magnetron transmitter, refractivity changes cannot reliably be achieved over periods greater than a few hours in the C band. Future tests will investigate the improvements obtained using a shorter pulse, which may allow retrieval over significantly longer periods to be achieved through a reduction in target location phase-change noise, as recommended in Nicol *et al.* (2013).

A new way of estimating the errors in the retrieved refractivity changes is proposed using the consistency of the individual estimates within the averaging area. Radar refractivity retrievals of 1 h changes can be obtained with retrieval errors between 0.7 and 1.4 *N* units within 30 km of the radar considered in this work. These errors in the radar refractivity estimates are consistent with the errors estimated from the accumulated changes over 24 h with respect to *in situ* observations. Operational forecast models at progressively higher resolutions are able to represent humidity structures at smaller scales that are closer to those observed by *in situ* measurements. However, the correlation of daily time series
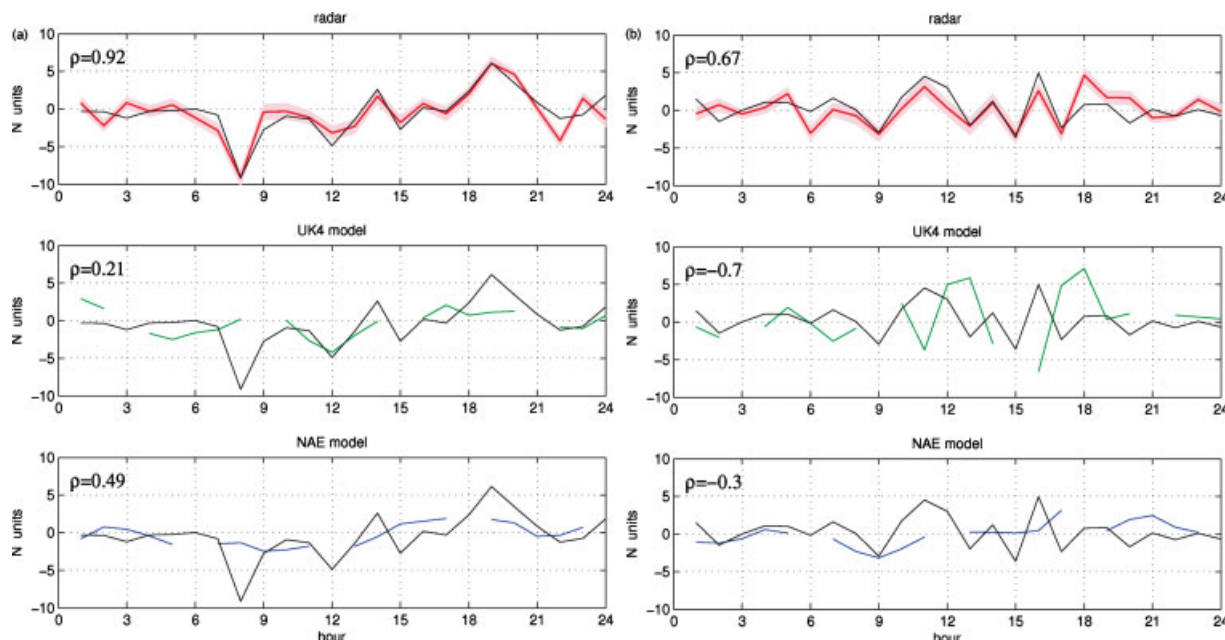
Figure 8. Time series of 1 h refractivity changes derived from *in situ* surface observations (black) compared with radar (red), the UK4 (4 km grid length) model (green) and the NAE (12 km grid length) model (blue) for (a) 2 March 2008 and (b) 1 August 2008. All data have been averaged on to a 12 km grid for comparison. The *in situ* observations are much more highly correlated with the radar observations than the values in the model.
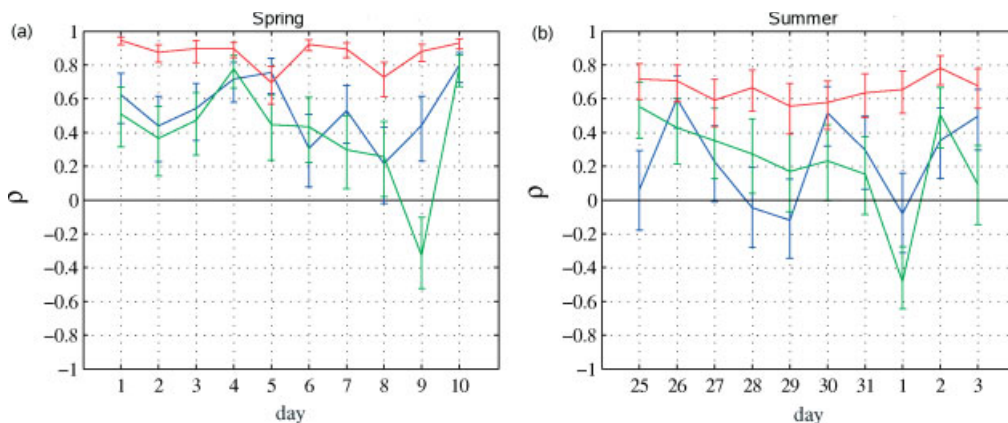

Figure 9. Daily correlations and 95% confidence intervals for 1 h refractivity changes of *in situ* surface observations in comparison with radar retrievals (red) and both UK4 (green) and NAE (blue) model output during (a) spring and (b) summer periods. Each point is the correlation derived from a 24 h time series as presented in Figure 8. All data have been averaged on to a 12 km grid for comparison. Consistently better agreement is obtained from radar retrievals than from either of the models.

of these model values of ΔN with *in situ* values is much lower than the correlation of the *in situ* values with the radar-derived values. The ability to resolve spatial patterns of significant refractivity (and therefore humidity) changes at a useful resolution suggests that radar refractivity retrievals may provide a useful data source for assimilation in NWP models to improve the representation of near-surface humidity, which may in turn improve forecasts of showers and convective storms.

Acknowledgements

References

Bartholomew K. 2012. '*Assessing the potential of radar refractivity retrievals for improved high resolution weather prediction*', PhD thesis, 178pp. Department of Meteorology, University of Reading: Reading, UK.

Bean BR, Dutton EJ. 1968. *Radio Meteorology*, *National Bureau of Standards Monograph, Vol. 92*, 435pp. National Bureau of Standards: Washington, D.C.

Bodine D, Michaud D, Palmer RD, Heinselman PL, Brotzge J, Gasperoni N, Cheong BL, Ming X, Gao J. 2011. Understanding radar refractivity: sources of uncertainty. *J. Appl. Meteorol. Climatol.* **50**: 2543–2560.

Crook NA. 1996. Sensitivity of moist convection forced by boundary layer processes to low-level thermodynamic fields. *Mon. Weather Rev.* **124**: 1767–1785.

Dabbert WF, Schlatter TW. 1996. Research opportunities from emerging atmospheric observing and modelling capabilities. *Bull. Am. Meteorol. Soc.* **77**: 305–323.

Davies T, Cullen J, Malcolm A, Mawson M, Staniforth A, White A, Wood N. 2005. A new dynamical core for the Met Office's global and regional modelling of the atmosphere. *Q. J. R. Meteorol. Soc.* **131**: 1759–1782.

Droegemeier KK, Smith JD, Businger S, Doswell III C, Doyle J, Duffy C, Foufoula-Georgiou E, Graziano T, James LD, Krajewski V, LeMone M, Lettenmaier D, Mass C, Pielke sr R, Rutledge S, Ray P, Schaake J, Zipser E. 2000. Hydrological aspects of weather prediction and flood warnings: Report of the ninth prospectus development team of the US Weather Research Program. *Bull. Am. Meteorol. Soc.* **81**: 2665–2680.

Emanuel K, Raymond D, Betts A, Bosart L, Bretherton C, Droegemeir K, Farrell B, Fritsch JM, Houze R, Lemone MA, Lilly D, Rotunno R, Shapiro M, Smith R, and Thorpe A. 1995. Report of the first prospectus development team of the US Weather Research Program to NOAA and the NSF. *Bull. Am. Meteorol. Soc.* **76**: 1194–1208.

Fabry F. 2004. Meteorological value of ground target measurement by radar. *J. Atmos. Oceanic Technol.* **21**: 560–573.

ⓒ 2013 The Authors. *Quarterly Journal of the Royal Meteorological Society* published by John Wiley & Sons Ltd on behalf of the Royal Meteorological Society.

Q. J. R. Meteorol. Soc. **140**: 1209–1218 (2014)

Fabry F. 2006. The spatial variability of moisture in the boundary layer and its effect on convection initiation: project-long characterization. *Mon. Weather Rev.* **134**: 79–91.

Fabry F, Frush C, Zawadski I, Kilambi A. 1997. On the extraction of near-surface index of refraction using phase measurements from ground targets. *J. Atmos. Oceanic Technol.* **14**: 978–987.

Fritsch JM, Houze Jr RA, Adler R, Bluestein H, Bosart L, Brown J, Carr F, Davis C, Johnson RH, Junker N, Kuo Y-H, Rutledge S, Smith J, Toth Z, Wilson JW, Zipser E, Zrnic D. 1998. Quantitative precipitation forecasting: report of the eighth prospectus development team, US Weather Research Program. *Bull. Am. Meteorol. Soc.* **79**: 285–299.

Hubbert JC, Dixon M, Ellis SM, Meymaris G. 2009. Weather radar ground clutter. Part I: identification, modelling and simulation. *J. Atmos. Oceanic Technol.* **26**: 1165–1180.

Koch S, Aksakal A, McQueen JT. 1997. The influence of mesoscale humidity and evapotranspiration fields on a model forecast of a cold-frontal squall line. *Mon. Weather Rev.* **125**: 384–409.

Lean H, Clark P. 2003. The effects of changing resolution on mesoscale modelling of line convection and slantwise circulations in FASTEX IOP16. *Q. J. R. Meteorol. Soc.* **129**: 2255–2278.

Lean HW, Clark PA, Dixon M, Roberts NM, Fitch A, Forbes R, Halliwell C. 2008. Characteristics of high-resolution versions of the Met Office Unified Model for forecasting convection over the United Kingdom. *Mon. Weather Rev.* **136**: 3408–3424.

Montmerle T, Caya A, Zawadzki I. 2002. Short-term forecasting of a shallow storms complex using bistatic and single-Doppler radar data. *Weather Forecast.* **17**: 1211–1225.

National Research Council. 1998. *The Atmospheric Sciences: Entering the Twenty-first Century.* National Academy Press: Washington, DC.

Nicol JC, Illingworth AJ. 2013. The effect of phase-correlated returns and spatial smoothing on the accuracy of radar refractivity retrievals. *J. Atmos. Oceanic Technol.* **30**: 22–39.

Nicol JC, Illingworth AJ, Darlington T, Sugier J. 2012. Techniques for improving ground clutter identification. In *Weather Radar and Hydrology*, Moore RJ, Cole SJ, Illingworth AJ. (eds.) Proceedings of the Exeter Symposium, April 2011: 45–51: IAHS Press: Wallingford, UK.

Nicol JC, Illingworth AJ, Darlington T, Kitchen M. 2013. Quantifying errors due to frequency changes and target location uncertainty for radar refractivity retrievals. *J. Atmos. Oceanic Technol.* **30**: 2006–2024.

Park S, Fabry F. 2010. Simulation and interpretation of the phase data used by the radar refractivity retrieval algorithm. *J. Atmos. Oceanic Technol.* **27**(8): 1286–1301.

Parsons DB, Shapiro MA, Miller E. 2000. The mesoscale structure of a nocturnal dryline and of a frontal-dryline merger. *Mon. Weather Rev.* **128**: 3824–3838.

Skolnik M. 1990. *Radar Handbook* (2nd edn). McGraw-Hill Inc: New York, NY.

Sun J. 2005. Convective-scale assimilation of radar data: progress and challenges. *Q. J. R. Meteorol. Soc.* **131**: 3439–3463.

Weckwerth TM, Wilson JW, Wakimoto RM. 1996. Thermodynamic variability within the convective boundary layer due to horizontal convective rolls. *Mon. Weather Rev.* **124**: 769–784.

Weckwerth TM, Parsons DB, Koch SE, Moore JA, LeMone MA, Demoz BB, Flamant C, Geerts B, Wang J, Feltz WF. 2004. An overview of the International H2O Project (IHOP_2002) and some preliminary highlights. *Bull. Am. Meteorol. Soc.* **85**: 253–277.

Weckwerth TM, Pettet CR, Fabry F, Park S, LeMone MA, Wilson JW. 2005. Radar refractivity retrieval: validation and application to short-term forecasting. *J. Appl. Meteorol.* **44**: 285–300.

Weldegaber MH, Demoz BB, Sparling LC, Hoff R, Chiao S. 2011. Observational analysis of moisture evolution and variability in the boundary layer during the dryline on 22 May 2002. *Meteorol. Atmos. Phys.* **110**: 87–102.

Xue M, Martin WJ. 2006a. A high-resolution modelling study of the 24 May 2002 dryline case during IHOP. Part I: numerical simulation and general evolution of the dryline and convection. *Mon. Weather Rev.* **134**: 149–171.

Xue M, Martin WJ. 2006b. A high-resolution modelling study of the 24 May 2002 dryline case during IHOP. Part II: horizontal convective rolls and convective initiation. *Mon. Weather Rev.* **134**: 172–191.

ⓒ 2013 The Authors. *Quarterly Journal of the Royal Meteorological Society* published by John Wiley & Sons Ltd on behalf of the Royal Meteorological Society.

Q. J. R. Meteorol. Soc. **140**: 1209–1218 (2014)